diversity

MDPI

Article

Foraging Environment Shapes the Gut Microbiota of Two Crane Species in the Yellow River Delta Wetland

Xiaodong Gao [1], Yunpeng Liu [2], Bo Zhou [2], Jingyi Yu [2], Lei Li [2], Qingming Wu [3], Jun Wang [2,*] and Shuai Shang [2,*]

[1] College of Life Sciences, Qufu Normal University, Qufu 273165, China; gao-xiaodong@163.com
[2] College of Biological and Pharmaceutical Engineering, Shandong University of Aeronautics, Binzhou 256600, China
[3] College of Wildlife and Protected Area, Northeast Forestry University, Harbin 150040, China
* Correspondence: ivywangjun@163.com (J.W.); shangshuai8983@126.com (S.S.)

Abstract

The foraging environment is a critical source of microbes for wild birds, yet its role in shaping the gut microbiota of sympatric crane species remains poorly understood. This study investigated this relationship in the Yellow River Delta wetland by analyzing the microbial communities of paired foraging environments and fecal samples from Common Cranes (*Grus grus*) and White Cranes (*Grus leucogeranus*) via 16S rRNA gene sequencing. Significant inter-group differences in alpha diversity (ACE, Chao1, Shannon, Simpson) indicated strong environmental filtering effects. Beta diversity (PCoA) revealed pronounced segregation between foraging and fecal samples (PC1 = 25.0%), underscoring a significant microbial turnover between the environment and the gut. Dominant phyla included Proteobacteria (24.6–37.4%), Firmicutes (4.8–29.0%), and Actinobacteriota (12.4–23.3%). LEfSe identified genus-level biomarkers highly specific to sample type and host, including *Ligilactobacillus* (12.1% in Common Crane feces) and *Cryobacterium* (9.2% in White Crane feces). SourceTracker analysis indicated that >70% of gut microbial sources remained unknown, suggesting a vast uncharacterized environmental reservoir. Functional prediction highlighted group-specific adaptations, such as elevated amino acid transport metabolism in Common Cranes (9.8% vs. 7.1%; $p < 0.05$), potentially linked to local dietary resources. Our findings demonstrate that the gut microbiota of cranes is synergistically shaped by host-specific factors and the unique saline–alkaline foraging environment of the wetland.

Keywords: gut microbiota; Yellow River Delta; 16S rRNA gene sequencing; microbial adaptation

Check for updates

Academic Editor: Michael Wink

Received: 18 November 2025
Revised: 20 December 2025
Accepted: 23 December 2025
Published: 25 December 2025

Copyright: © 2025 by the authors. Licensee MDPI, Basel, Switzerland. This article is an open access article distributed under the terms and conditions of the Creative Commons Attribution (CC BY) license.

1. Introduction

As one of the most complex micro-ecosystems in animals, intestinal microbiota is essential in maintaining host health, regulating metabolism, and enhancing environmental adaptability [1,2]. In recent years, it has become a key focus in interdisciplinary research. Evidence suggests that the intestinal microbiota profoundly influences animals' physiological functions and ecological adaptation strategies through nutrient metabolism, immune regulation, and interactions between the host and its environment. The gut microbiota is frequently characterized as a crucial "microbial organ" within an organism, and the symbiotic entity comprising the host animal and its microbiota is termed a "holobiont" [3]. Birds represent a highly successful group of organisms, exhibiting remarkable species and genetic diversity [4]. In comparison to mammals, the gut microbiota of birds is characterized by relatively lower stability and greater plasticity [5]. Wild birds exhibit a wide range

of dietary preferences, flight behaviors, and developmental strategies [6], which contribute to the complexity of their intestinal microbiota. Changes in the intestinal microbiota of wild birds have significant effects on the host's physiological characteristics, nutritional status, and stress response [7]. Recent studies on *Ficedula hypoleuca* and other small passerines have highlighted pronounced fine-scale variation driven by microhabitat, season and individual identity [8–10]. The dynamic regulation of the intestinal microbiota is frequently considered a key mechanism by which birds enhance their ecological adaptability [11].

The common crane (*Grus grus*) is a large migratory bird species with a wide distribution across wetland ecosystems in Eurasia. As a flagship species for wetland ecosystems, its survival status directly indicates habitat quality. In China, the common crane exhibits extensive distribution. During its migration period, it is commonly observed in most provincial-level administrative regions, particularly in the Yellow River Delta and the Yangtze River Basin [12]. Its breeding grounds are primarily in northern Xinjiang, Inner Mongolia, and Heilongjiang. At the same time, wintering areas are predominantly distributed across the Yellow River Basin, the middle and lower reaches of the Yangtze River, and the Yunnan-Guizhou Plateau. Driven by global climate change, wintering ranges have shown a significant trend of expanding northward. In recent years, substantial wintering populations have been recorded in regions extending beyond the Yellow River Delta, including southern parts of Northeast China. As China's largest newly formed wetland, the Yellow River Delta possesses a unique saline–alkaline environment and water-sediment dynamics that significantly influence the food chain structure of the common crane's habitat. Studies indicate that the salinity gradient within the wetland markedly affects the soil microbial community, which propagates through the food chain to impact avian gut microbiota. For instance, a high-salinity environment suppresses the activity of nitrifying bacteria, potentially reducing nitrogen availability in wetland vegetation and indirectly affecting food quality for common cranes. Moreover, recent ecological water replenishment initiatives in the Yellow River Delta, such as water-sediment regulation, have substantially enhanced wetland vegetation coverage.

The intestinal microbiota plays a pivotal role in digestion and absorption, immune regulation, and environmental adaptation in the common crane. For example, it assists the host in adapting to seasonal dietary shifts and migratory stress by degrading plant fibers, synthesizing essential nutrients such as short-chain fatty acids, and resisting pathogenic microorganisms. Recent studies have demonstrated that the common crane's intestinal microbiota diversity is closely associated with its dietary composition and habitat environment. Notably, there are marked differences in microbiota composition between wild and semi-captive populations, highlighting the significant influence of environmental factors on microbiota regulation. The resurgence of salt-tolerant plants like *Suaeda salsa* has provided abundant food resources for common cranes and may modulate their gut flora by enhancing dietary diversity. The stability of the intestinal microbiota in common cranes is susceptible to various environmental challenges. In particular, saline–alkaline stress exerts a substantial impact, as soil salinity in the Yellow River Delta affects the microbial community ingested by the common crane through the food chain.

2. Materials and Methods

2.1. Study Area and Sample Collection

The samples for this study were collected from the 1200 Forest Farm area within the Yellow River Delta National Nature Reserve (38°3′57″ N, 118°45′57.29″ E). All samplings occurred within a defined, observable radius (<1 km) from this central point across uniform estuarine riverbank and farmland habitats frequented by foraging cranes. This region features diverse wetland habitats, including estuarine rivers, muddy tidal flats, and rota-

tional farmlands, which provide extensive foraging and resting grounds for cranes. During the winter season, the area is primarily inhabited by Common Cranes and White Cranes, whose populations are relatively dispersed. During sample collection, the research team was split into two groups. One group was responsible for monitoring White Cranes, while the other monitored Common Cranes. The sampling process primarily focused on observing foraging behavior and defecation events. Immediately after observing the foraging activities of cranes in farmland areas, foraging samples (consisting of soil and residual vegetation) were gathered. Likewise, fecal samples were collected right after defecation was witnessed (usually, the collection was completed within 5 min). To establish a connection between foraging and fecal samples from the same crane population, samples were collected within spatially and temporally related contexts. Specifically, foraging samples were taken from the immediate ground area where a particular, observed flock had been actively foraging for more than 10 min, and subsequent fecal samples were collected from the same flock within the same hour and within a radius of 200 m. Sterile sampling tubes were used throughout collection, and disposable sterile gloves were changed between samples to avoid cross-contamination. A total of six replicate samples were gathered for each category: foraging samples of Common Cranes (DYH1–6), fecal samples of Common Cranes (DYHT1–6), fecal samples of White Cranes (DYB1–6), and foraging samples of White Cranes (DYBT1–6). To avoid cross-contamination, collectors donned new disposable nitrile gloves for each sample, and tools were disinfected with 75% ethanol between uses. The ambient temperature during the collection process ranged from 1 °C to 5 °C. Samples were promptly placed in a portable freezer maintained at −20 °C on dry ice, transported to the laboratory within 4 h, and then stored at −80 °C. The duration of storage at −20 °C during transportation and before transfer to −80 °C was less than 48 h.

2.2. Sample Treatment

In this study, 0.3 g of each sample was precisely weighed. Total DNA extraction from fecal samples was conducted using the TIANamp Stool DNA Kit (TianGen Biotech (Beijing) Co., Ltd., Beijing, China). The concentration and purity of the extracted DNA were evaluated using a NanoDrop 2000 spectrophotometer (Thermo Fisher Scientific, Waltham, MA, USA). Subsequently, PCR amplification was performed with primers 515F (5′-GTGCCAGCMGCCGCGG-3′) and 907R (5′-CCGTCAATTCMTTTRAGTTT-3′) to construct the sequencing library [13]. PCR reactions, with a total volume of 25 μL, were composed of 12.5 μL of 2× KAPA HiFi HotStart ReadyMix (San Diego, CA, USA), 1 μL of each primer at a concentration of 5 μM, 1 μL of template DNA, and 9.5 μL of nuclease-free water. The thermal cycling conditions were set as follows: an initial denaturation step at 95 °C for 3 min; followed by 30 cycles, each consisting of 30 s at 95 °C, 30 s at 55 °C, and 30 s at 72 °C; and a final extension step at 72 °C for 5 min. Amplicon libraries were prepared using the NEBNext® Ultra™ II DNA Library Prep Kit (New England Biolabs, Ipswich, MA, USA) and then quantified. Paired-end sequencing with a read length of 2 × 250 bp was carried out on an Illumina NovaSeq 6000 platform (San Diego, CA, USA) provided by Biomarker Technologies Co., Ltd. (Beijing, China). The raw image data files generated during high-throughput sequencing were processed through base calling to yield raw sequencing reads, which were stored in FASTQ format (18 January 2025).

2.3. Data Analysis

Raw sequencing reads were quality-filtered and denoised using the DADA2 plugin (callahan 2016 dada2) within QIIME2 version 2020.6 [14,15]. The QIIME software generated species abundance tables at various classification levels (SILVA138 database, version 2019-12-16). At the same time, the R programming language (12 January 2024) was used

to visualize the community structure diagrams of each sample across different taxonomic levels. For diversity analyses, ASV tables were rarefied to a depth of 35,000 sequences per sample to standardize sampling effort. Alpha diversity reflects the species richness and evenness within a single sample. Several metrics, including Chao1, Shannon, Simpson, and Coverage, are commonly used to quantify alpha diversity. The Chao1 and Ace indices specifically estimate species richness, which refers to the sample's total number of distinct species. In contrast, the Shannon and Simpson indices measure species diversity, considering both species richness and the evenness of their distribution within the community. Alpha diversity metrics, namely Chao1 and Shannon, were calculated and compared through Kruskal–Wallis tests. Beta diversity was evaluated using Bray–Curtis dissimilarity. A permutational multivariate analysis of variance (PERMANOVA, with 999 permutations) was carried out using the adonis2 function to examine group differences. Under conditions of equal species richness, greater evenness among species leads to higher overall diversity. Higher values of the Shannon and Simpson indices indicate increased species diversity within the sample [16]. Beta diversity analysis was performed using the QIIME software to assess and compare species diversity similarity across different samples. Principal Component Analysis (PCoA based on Bray–Curtis distances) was used to analyze and simplify complex datasets by decomposing variance and representing the differences among multiple sets of data on a two-dimensional coordinate graph [17]. The PCoA analysis graphs were generated using the R language tool (ggplot 3.1.1).

3. Results

3.1. Sequence Statistics and ASV Cluster Analysis

1,808,455 paired-end reads were obtained from the sequencing of 24 samples. Following quality control and assembly, 1,611,112 clean reads were generated, with each sample producing no fewer than 35,712 clean reads and an average of 67,130 clean reads per sample. Specifically, the DYB group yielded 336,983 clean reads, the DYBT group yielded 425,181 clean reads, the DYH group yielded 422,278 clean reads, and the DYHT group yielded 426,730 clean reads. In this study, a total of 58,205 ASVs were identified across four groups. A high number of ASVs is common in environmental and wildlife samples due to the high microbial diversity and the sensitivity of the DADA2 algorithm in resolving single-nucleotide differences. To reduce the potential bias introduced by sequencing errors or extremely rare taxa, we applied a prevalence filter, retaining only ASVs that were present in at least two samples. This common conservative approach enhances the robustness of downstream ecological analyses by focusing on more consistently detectable microbial features. To ensure biological relevance, we focused our analysis on ASVs that were present in at least two samples with a total abundance of >10 reads. The data quality is evaluated by systematically analyzing the number of sample sequences across each stage of the statistical process. This evaluation primarily entails conducting a detailed statistical analysis of various parameters, such as the number of sequences and sequence length (Figure 1).

Specifically, 11,826, 13,067, 19,888, and 19,369 ASVs were detected in the DYB, DYH, DYHT, and DYBT groups. Furthermore, 895 common ASVs were shared between the DYB and DYH groups; 2887 common ASVs were identified between the DYHT and DYBT groups; 1092 common ASVs were observed between the DYH and DYHT groups; 832 common ASVs were found between the DYB and DYBT groups; and 218 common ASVs were present across all four groups.

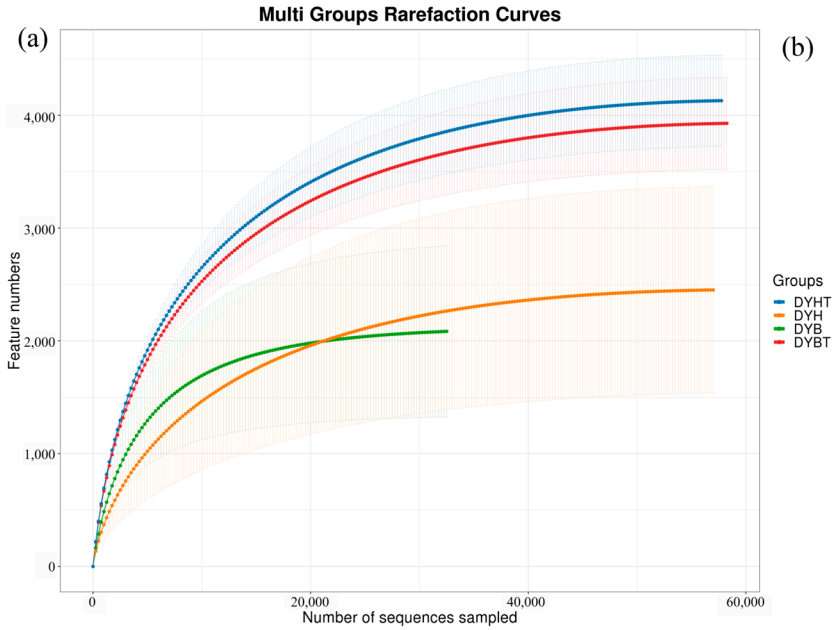


Figure 1. Sequence statistics and ASV cluster analysis. Note: (**a**) means Rarefaction curves among different groups; (**b**) means ASV among different groups. DYH: foraging samples of Common Cranes; DYHT: fecal samples of Common Cranes; DYB: fecal samples of White Cranes; DYBT: foraging samples of White Cranes.

3.2. α-Diversity Analysis of the Microbiota Among Four Groups

The image compares alpha diversity indices comprehensively across four distinct groups (DYHT, DYH, DYB, and DYBT) using four box-and-whisker plots. Each plot corresponds to a specific diversity index: ACE (Figure 2a), Chao1 (Figure 2b), Shannon (Figure 2c), and Simpson (Figure 2d), with Student's *t*-test employed to assess statistical significance. The ACE index plot (Figure 2a) reveals significant differences between groups, with *p*-values such as 0.0045 (DYHT vs. DYH) and 0.00061 (DYB vs. DYBT), indicating notable variations in species richness. Similarly, the Chao1 index plot (Figure 2b) demonstrates comparable *p*-values (e.g., 0.0046), reinforcing the observed disparities in community richness. The Shannon index plot (Figure 2c), reflecting species richness and evenness, exhibits *p*-values like 0.0034, suggesting significant differences in diversity. The Simpson index plot (Figure 2d), focusing on dominance, shows *p*-values such as 0.012, highlighting variations in community dominance structures. The y-axes are scaled according to each index: the Shannon index ranges approximately from 7 to 12, while the Simpson index spans from 0.96 to 1.00, indicating high evenness across groups. The ACE and Chao1 plots emphasize richness differences, whereas Shannon and Simpson plots integrate evenness, providing a holistic view of alpha diversity. The consistent use of Student's *t*-test underscores rigorous statistical validation. The visual clarity of the 2 × 2 grid facilitates cross-index comparisons, revealing that DYHT and DYH often exhibit more pronounced differences (e.g., $p < 0.005$) compared to other group pairs. This structured presentation effectively communicates the heterogeneity in microbial or ecological communities across the four experimental conditions, making it a robust visual aid for diversity analysis.

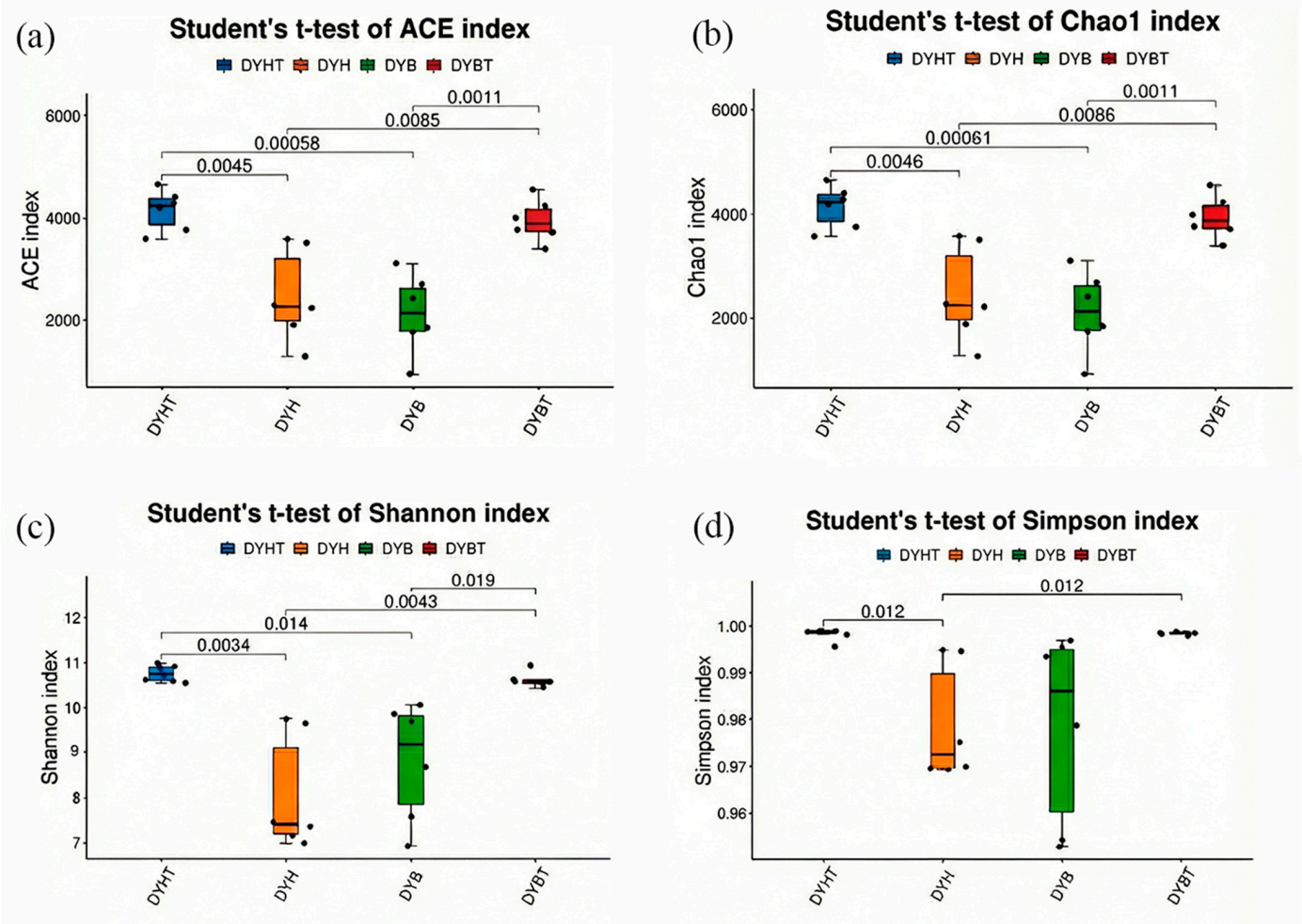


Figure 2. α-diversity analysis of the microbiota among four groups. Note: The x-axes label the four groups, distinguished by colors (blue: DYHT, orange: DYH, green: DYB, red: DYBT). Each box represents the interquartile range (IQR), with the median marked inside and whiskers extending to non-outlier data extremes. The layout is meticulously organized, with clear titles, annotations, and *p*-values above relevant comparisons. Note: (**a**) means ACE index; (**b**) means Chao1 index; (**c**) means Shannon index; (**d**) means Simpson index. DYH: foraging samples of Common Cranes; DYHT: fecal samples of Common Cranes; DYB: fecal samples of White Cranes; DYBT: foraging samples of White Cranes.

3.3. β-Diversity Analysis of the Microbiota Among Four Groups

The figure presents a comprehensive analysis of microbial community structure across multiple sample groups (DYB, DYH, DYHT and DYBT) through two complementary analytical approaches.The combination of these approaches provides robust evidence for group-specific microbial signatures, with the PCoA particularly highlighting the strong separation between DYH and DYHT communities. This integrated visualization effectively communicates both taxonomic and ecological dimensions of microbial community variation across the experimental groups(Figure 3a). In Figure 3b, the left panel displays a hierarchical clustering dendrogram based on community similarity, revealing distinct sample groupings (DYB, DYH, DYHT and DYBT). The right panel illustrates the relative abundance of microbial taxa through stacked bar charts, where dominant genera include *Sphingomonas*, *Rhodococcus*, *Pseudomonas*, and other taxa such as *Arthrobacter*, *Cryobacterium*, and *Ligilactobacillus*. The plot coordinates indicate specific sample positions, demonstrating that DYH samples cluster in the upper-left quadrant. In contrast, DYHT samples occupy the lower-right region, suggesting distinct community structures between these groups.

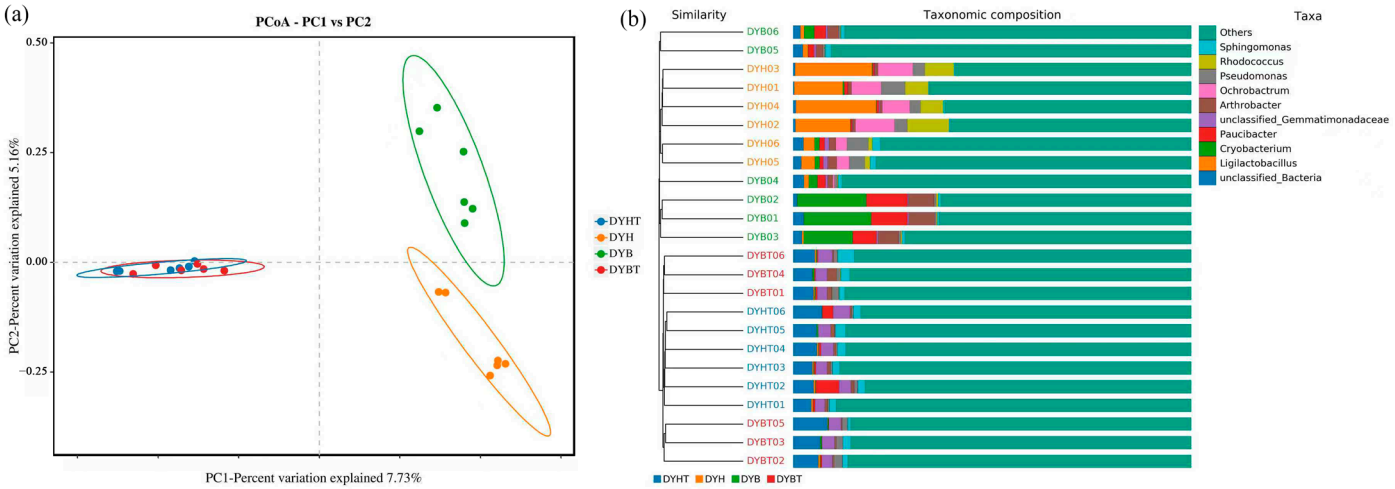


Figure 3. β-diversity analysis of the microbiota among four groups. Note: (**a**) means presents a PCoA plot based on Bray–Curtis dissimilarity, with principal coordinate 1 (PC1) explaining 25.00% of the variation and PC2 representing additional variance. Samples are segregated by group with confidence ellipses emphasizing group-specific clustering patterns. (**b**) means combines hierarchical clustering with taxonomic composition analysis. DYH: foraging samples of Common Cranes; DYHT: fecal samples of Common Cranes; DYB: fecal samples of White Cranes; DYBT: foraging samples of White Cranes.

3.4. Analysis of Microbial Composition Characteristics

The figure presents a comparative analysis of bacterial community composition across four experimental groups (DYHT, DYH, DYB, DYBT) through two vertically stacked bar charts (Figure 4), each illustrating the relative abundance of microbial taxa at different taxonomic resolutions. Our results showed that the relative abundance (as proportions) of various bacterial phyla across four samples (Figure 4a): DYHT, DYH, DYB, and DYBT. Proteobacteria is the dominant phylum in DYHT (30.44%), DYH (37.42%), and DYBT (35.06%), but in DYB, Firmicutes has the highest abundance (28.98%), while Proteobacteria drops to 24.61%. Firmicutes shows significant variability, being relatively low in DYHT (5.68%) and DYBT (4.75%) but substantially higher in DYH (25.00%) and DYB (28.98%). Actinobacteriota maintains moderate levels across all samples, peaking in DYH (23.13%) and DYB (23.31%), but decreases in DYBT (12.44%). Bacteroidota, Chloroflexi, Acidobacteriota, and other minor phyla generally exhibit lower abundances with minimal fluctuations; for instance, Bacteroidota ranges from 3.91% in DYH to 12.05% in DYBT. Overall, the data reveals sample-specific shifts, such as the prominence of Firmicutes in DYB contrasting with Proteobacteria dominance elsewhere, potentially indicating environmental or experimental influences on microbial community structure. We analyzed the relative abundance of bacterial genera (Figure 4b) across the same four samples (DYHT, DYH, DYB, DYBT). The most striking observation is the highly variable dominance of specific genera in different samples. In the DYH group, *Ligilactobacillus* was exceptionally abundant (12.10%), far exceeding its presence in other samples (0.21–0.62%). Conversely, *Cryobacterium* dominates in the DYB group (9.18%), while its abundance is much lower elsewhere (0.18–0.29%). DYH also showed significant enrichment of *Ochrobactrum* (6.58%) and *Rhodococcus* (5.37%), genera present at very low levels (<0.06% and <0.26%, respectively) in the other samples. The *Paucibacter* was notably high in DYB (5.55%) compared to others (<1.68%). While *Pseudomonas* is moderately abundant in the DYH (4.03%) and DYBT group (1.45%), and Arthrobacter peaks in the DYB group (4.07%). Overall, the data reveals dramatic sample-specific enrichment of particular genera (*Ligilactobacillus* in DYH, *Cryobacterium* and *Paucibacter* in DYB, *Ochrobactrum* and *Rhodococcus* in DYH), suggesting that distinct environmental conditions

or selective pressures may be associated with differences in the microbial communities of each sample.

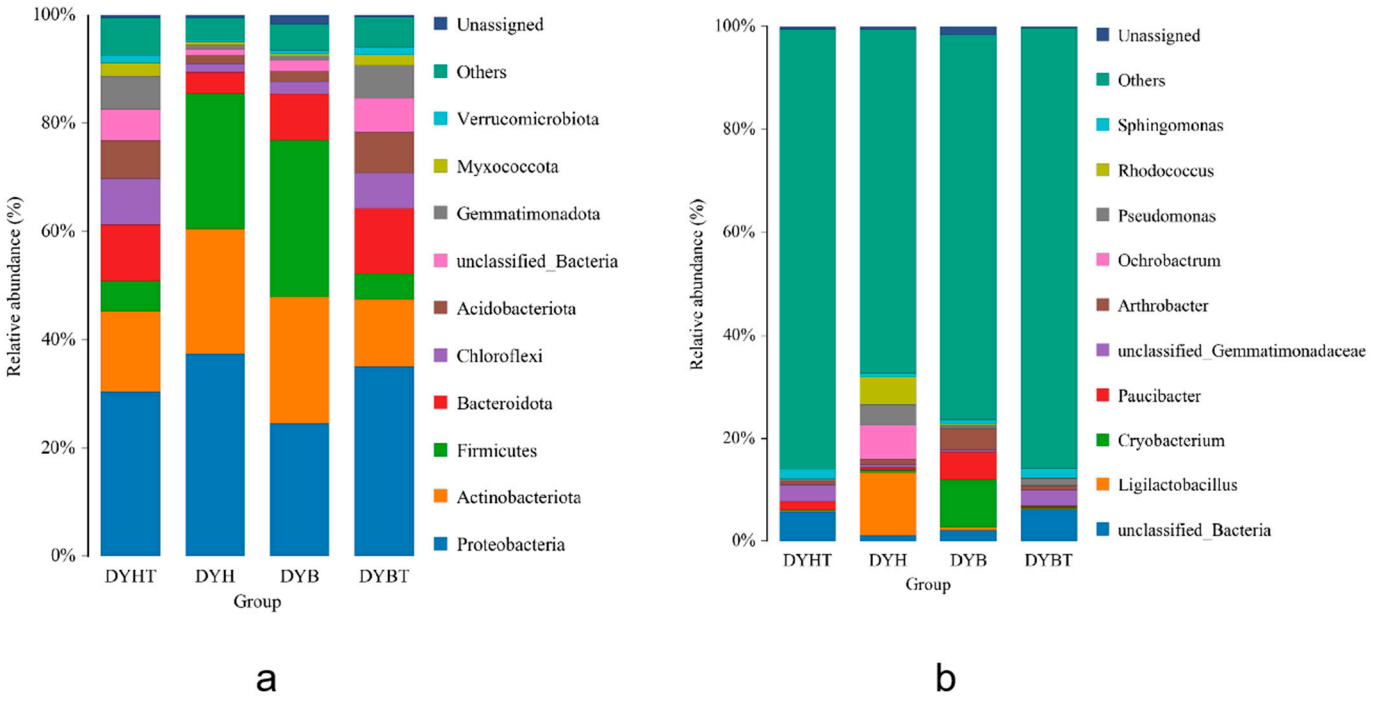


Figure 4. Analysis of microbial composition characteristics among four groups. Note: (**a**) means microbial composition at the phyla level; (**b**) means microbial compositon at the genus level. DYH: foraging samples of Common Cranes; DYHT: fecal samples of Common Cranes; DYB: fecal samples of White Cranes; DYBT: foraging samples of White Cranes.

3.5. SourceTracker Analysis

The figure presents a comparative source-tracking analysis between DYB vs. DYBT (Figure 5a) and DYH vs. DYHT (Figure 5b) microbial communities. The stacked bar charts reveal that the "Unknown" source (blue) dominates across all samples (DYB_DYB01-06, DYH_DYH01-06), consistently exhibiting higher relative abundance (bar height) than the target sources DYBT (red, Figure 5a) or DYHT (red, Figure 5b). This pattern suggests a limited contribution from the hypothesized sources (DYBT/DYHT) to the respective microbial communities. The systematic arrangement of sample pairs facilitates direct comparison, demonstrating that while trace amounts of DYBT/DYHT signatures are detectable (minor red segments), the predominant microbial origins remain uncharacterized ("Unknown"). These results indicate insufficient reference database coverage or substantial compositional divergence between the target sources and analyzed communities.

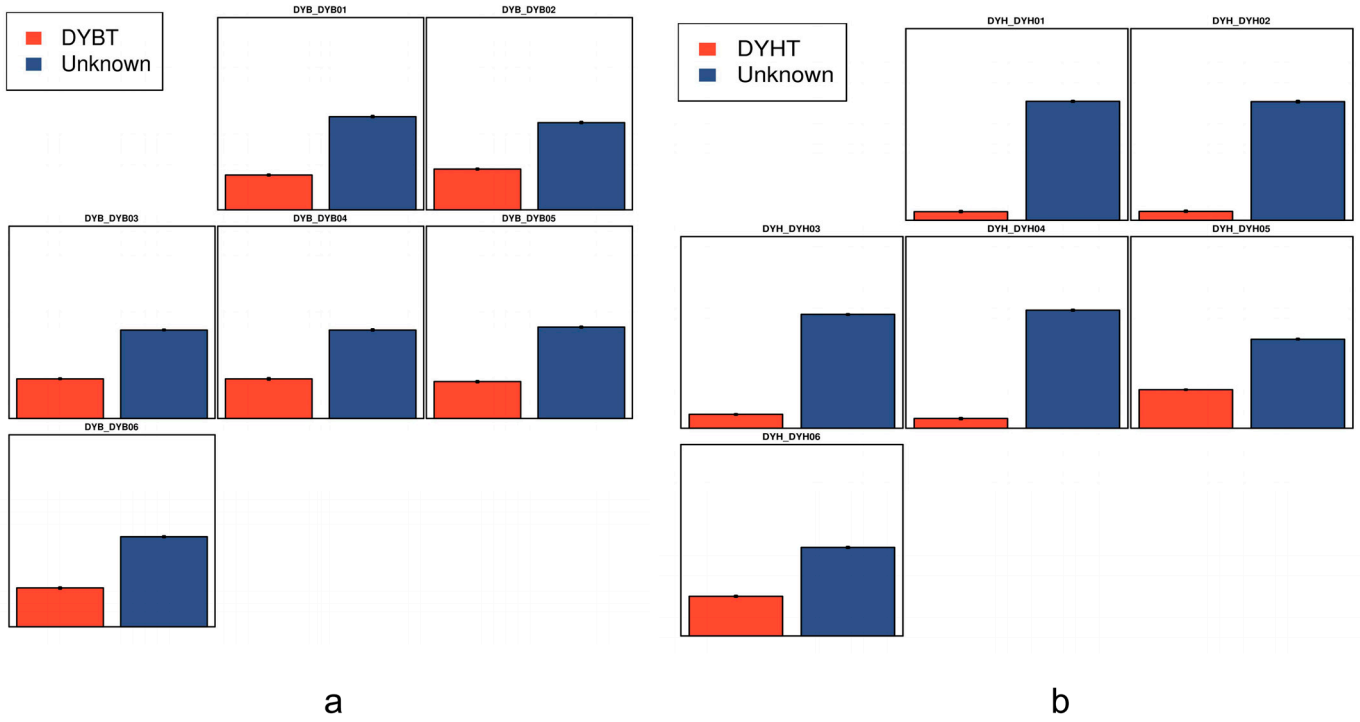


Figure 5. SourceTracker analysis among four groups. Note: (**a**) means source-tracking analysis between DYB vs. DYBT; (**b**) means source-tracking analysis between DYH vs. DYHT. DYH: foraging samples of Common Cranes; DYHT: fecal samples of Common Cranes; DYB: fecal samples of White Cranes; DYBT: foraging samples of White Cranes.

3.6. LEfSe Analysis

LEfSe is a robust bioinformatics tool developed to identify biomarkers demonstrating statistically significant differences across multiple biological groups. This approach combines non-parametric statistical tests, specifically the Kruskal–Wallis rank-sum test and pairwise Wilcoxon rank-sum tests, with linear discriminant analysis (LDA) to estimate the effect size of differentially abundant features. In analyzing microbial communities across four distinct groups, LEfSe facilitates the detection of both taxonomic clades and individual species that consistently distinguish one group from others (Figure 6). LEfSe analysis identified distinct microbial signatures across the four groups in this study. Specific phyla (e.g., Actinobacteria, Firmicutes) and genera (e.g., *Lactobacillus*, *Bifidobacterium*) were found to dominate specific clusters, indicating their potential roles as biomarkers for group stratification (Figure 6). The Chloroflexi, Gemmatimonadota, and Myxococcota served as key supporting phyla for the DYHT group; the Proteobacteria and Actinobacteriota supported the DYH group; the Bacteroidota and Acidobacteriota supported the DYBT group; and the Firmicutes supported the DYB group. At the genus level, *Ligilactobacillus*, *Ochrobactrum*, *Rhodococcus*, *Catellicoccus*, *Pseudomonas*, *Microbacterium*, *Microbulbifer*, and *Pseudorhizobium* were important supporting genera for the DYH group; *Lysobacter* was a key supporting genus for the DYBT group; Paucibacter, Enterococcus, Arthrobacter, and Bacillus were critical supporting genera for the DYB group.

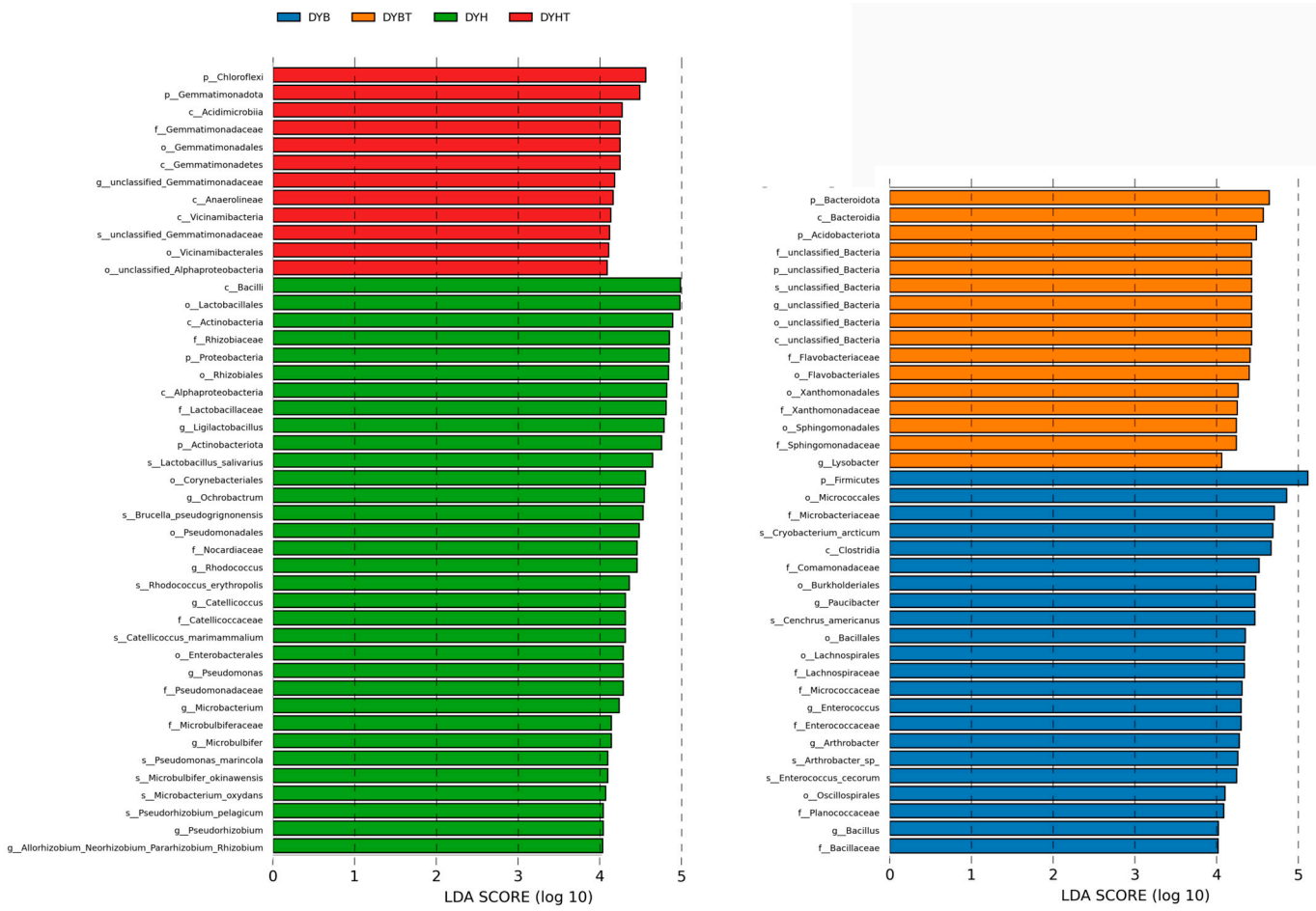


Figure 6. LEfSe analysis among four groups. DYH: foraging samples of Common Cranes; DYHT: fecal samples of Common Cranes; DYB: fecal samples of White Cranes; DYBT: foraging samples of White Cranes.

3.7. Functional Predictive Analysis

The figure presents a comprehensive comparative analysis of functional gene category distributions across four experimental groups (DYH, DYB, DYHT, DYBT) through three systematically organized panels (Figure 7a–c), each employing a dual-plot design to visualize relative abundances and statistically significant differences simultaneously. Figure 7a contrasts DYH (blue bars) and DYB groups, revealing that "Function unknown" represents the most abundant category (15.2% mean proportion), followed by "Translation, ribosomal structure, and biogenesis" (12.8%), with statistically significant differences observed in "Signal transduction mechanisms" and "Coenzyme transport and metabolism." The right-side dot plots with 95% confidence intervals quantitatively demonstrate these inter-group variations, where positive values indicate DYH predominance and negative values reflect DYB dominance in specific functional categories.

Figure 7b compares DYHT and DYH groups, showing distinctive metabolic profiles with "Secondary metabolites biosynthesis" exhibiting the most pronounced difference and "Cell wall/membrane biogenesis" showing substantial variation. Notably, "Defense mechanisms" display a consistent 8.5% mean proportion across groups, while "Carbohydrate transport and metabolism" maintains stable abundance, suggesting conserved metabolic functions. The statistical annotations reveal moderate evidence for differences, with confidence intervals spanning 1.5–3.2% difference magnitudes.

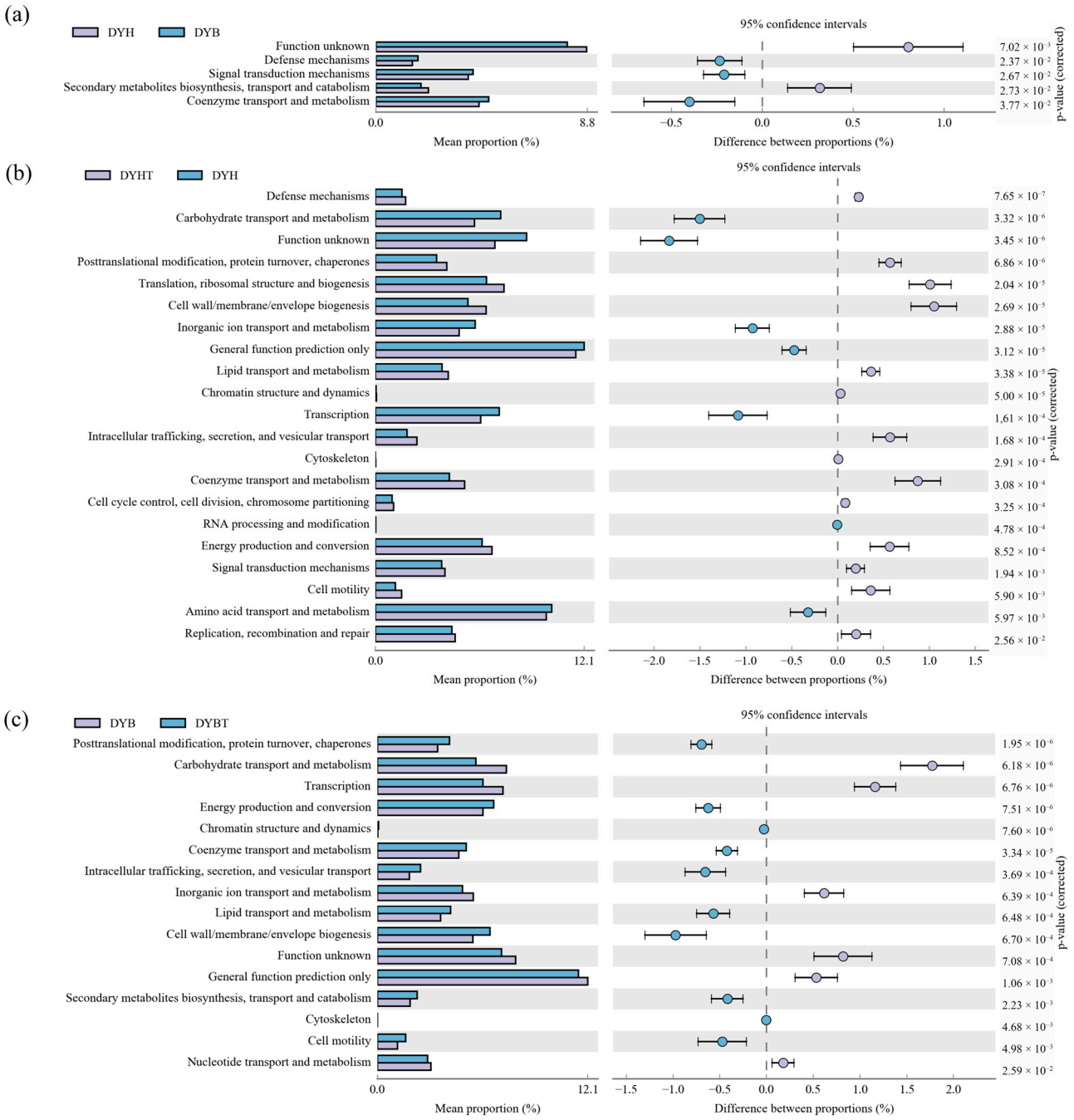


Figure 7. Functional predictive analysis among different groups. Note: (**a**) means DYH vs DYB; (**b**) means DYHT vs DYH; (**c**) means DYB vs DYBT. DYH: foraging samples of Common Cranes; DYHT: fecal samples of Common Cranes; DYB: fecal samples of White Cranes; DYBT: foraging samples of White Cranes.

Figure 7c provides critical insights into DYB versus DYBT comparisons, where "Posttranslational modification" emerges as the dominant functional category (18.3% mean proportion), followed by "Carbohydrate transport and metabolism" (10.1%). The most statistically robust difference occurs in "Energy production and conversion" ($p = 7.02 \times 10^{-3}$), with DYBT showing enhanced functionality. The visualization employs a standardized y-axis (0–20% proportion range) across all panels, facilitating cross-comparison of 18+ functional categories, including "Nucleotide transport and metabolism" (6.2–7.5%) and "Intracellular trafficking" (4.8–5.3%). The minimalist color scheme (blue for proportions, grey for differences) and consistent layout enhance interpretability, while the

integrated presentation of mean proportions and statistical significance ($p < 0.05$ indicated for 7/18 categories) provides a robust framework for understanding how experimental conditions shape functional potential in microbial communities. This analytical approach effectively reveals group-specific metabolic signatures, particularly the elevated "Amino acid transport" in DYH (9.8%) versus DYBT (7.1%) and specialized functions like "Chromatin structure and dynamics" showing differential expression patterns.

4. Discussion

As a complex micro-ecosystem, the intestinal microbiota plays a pivotal role in maintaining host health, regulating metabolism, and improving environmental adaptability. In wild birds, the assembly of the microbiota is affected by a variety of biotic and abiotic factors, such as diet, anthropogenic disturbance, seasonality, geographic context, and exposure to environmental microbes [18–21]. Our study centered on the gut microbiota of two sympatric crane species in the Yellow River Delta, a crucial wetland habitat undergoing substantial environmental transformation, to analyze how foraging environments and host factors interact to mold microbial communities. Notably, alpha diversity indices (ACE and Chao1) exhibited significant disparities between fecal samples of Common Cranes (DYHT) and their foraging samples (DYH) ($p < 0.005$), highlighting a potent environmental filtering effect. This pattern is consistent with a scenario of strong environmental filtering or selective host retention, although our observational design cannot distinguish between these processes. This observation aligns with the recognized plasticity of avian gut microbiota [5,22]. High Shannon and Simpson indices observed across all groups further reflect a considerable level of microbial diversity and evenness, which is likely attributable to the cranes' diverse diet and heterogeneous wetland habitats. The beta diversity analysis further substantiated the pronounced segregation between foraging and fecal samples. Specifically, the Principal Coordinate Analysis (PCoA) highlighted an appreciable variance (PC1 = 25.0%) that was driven by foraging behavior and digestive processes. The PERMANOVA test confirmed that this sample type-driven clustering was statistically significant ($p < 0.01$, $R^2 = 0.18$), indicating a meaningful effect. These results are consistent with the interpretation that environmental substrates are a major contributor to the crane gut microbiota, alongside host-specific factors. However, the substantial proportion of variance explained by other factors, including the large "unknown" source identified in our SourceTracker analysis, underscores the significant contribution of unmeasured variables such as specific dietary components, individual host physiology, and potential vertical transmission.

Consistent with other avian studies [23,24], dominant phyla included Proteobacteria, Firmicutes, Actinobacteriota, and Bacteroidota. The prevalence of Proteobacteria may reflect their ecological versatility and stress tolerance, advantageous in dynamic wetland settings [25]. Firmicutes and Actinobacteriota play established roles in energy harvest and organic matter degradation [23,26–28], suggesting functional adaptation to local diet and sediment characteristics. Importantly, the dominance of these phyla in both foraging and fecal samples implies strong environmental inoculation followed by host selection. Thus, the high abundance of Proteobacteria may be related to their ability to adapt to various environmental stresses [25], while Actinobacteriota and Firmicutes play essential roles in nutrient metabolism and immune regulation. At the genus level, *Ligilactobacillus*, *Rhodococcus*, *Pseudomonas*, and *Sphingomonas* were identified as discriminant key genera in different groups. For example, *Ligilactobacillus* was a key discriminant biomarker for the DYH group in our analysis, possibly related to the common crane's adaptation to a plant-rich diet. However, we note that the identification of such biomarkers is preliminary given the sample size and requires validation in larger cohorts. Rhodococcus has been reported to be able to degrade hydrocarbons and other pollutants, suggesting that it may

play a role in detoxifying environmental toxins in the intestinal tract of cranes, a hypothesis that warrants future targeted investigation.

LEfSe analysis further confirmed microbial signatures tied to sample type and species. For instance, Chloroflexi and Myxococcota were indicative of foraging sites, reinforcing that sediment and soil microbiomes contribute significantly to gut community assembly. The functional predictions align with ecological context: elevated amino acid transport metabolism in Common Cranes may counterbalance limited dietary protein in winter, while conserved defense mechanisms (8.5%) across groups suggest non-negotiable immune protection in pathogen-rich wetlands. The ongoing ecological water replenishment projects in the Yellow River Delta have revitalized native vegetation like Suaeda salsa, potentially enriching food resources and thereby microbial diversity. This underscores the value of habitat restoration not only for crane foraging but also for maintaining microbiome-mediated health. Furthermore, the sensitivity of the crane microbiota to environmental quality positions it as a promising bio-indicator for wetland ecosystem monitoring.

We explicitly acknowledge key limitations in causal inference. The sample size (n = 6 per group), though typical in wildlife studies, may have limited power to capture full within-group variation. Furthermore, samples were collected during a single season; thus, our findings may not fully represent the dynamics of Intestinal microorganisms across different under varying seasonal environmental conditions. Additionally, the high proportion of unclassified microbes (mean 12.4%) reflects database biases against environmental and wetland-associated taxa, affecting SourceTracker accuracy. It is also important to note that the functional profiles inferred from 16S rRNA gene data are predictive and based on phylogenetic imputation and database annotations; hence, they cannot directly measure expressed microbial functions, representing a constraint on functional interpretation. Future work should employ metagenomics or culturomics to improve taxonomic resolution and functional inference.

5. Conclusions

In conclusion, this study elucidates how the interplay between host foraging behavior and wetland environmental conditions shape the gut microbiota of two crane species. Our findings underscore the role of ambient microbial reservoirs in gut community assembly and offer a scientific basis for integrated microbial and environmental conservation strategies. Future studies should expand sample sizes, include temporal monitoring, and incorporate metabolomic and environmental chemical data to fully unravel microbial feedback mechanisms in wetland health.

Author Contributions: S.S., X.G. and Y.L.: conceptualization, methodology, investigation, and writing—original draft preparation. L.L.: software. X.G.: validation. B.Z.: formal analysis. J.Y.: resources. S.S.: data curation. Q.W. and J.W.: writing, review, and editing. Q.W.: supervision, project administration, funding, and acquisition. All authors have read and agreed to the published version of the manuscript.

Funding: The Chongqing Technological Innovation and Application Development Special Project (CSTB2024TIAD-LDX0019). National Key Research and Development Program of China (2023YFF1305000), and the National Natural Science Foundation of China (32271557).

Institutional Review Board Statement: Not applicable.

Data Availability Statement: The data presented in this study are openly available in NCBI (https://www.ncbi.nlm.nih.gov/, accessed on 22 December 2025), reference number SAMN50429475-50429498 (PRJNA1300859).

Conflicts of Interest: The authors declare no conflicts of interest.

References

1. Baeckhed, F.; Ley, R.E.; Sonnenburg, J.L.; Peterson, D.A.; Gordon, J.I. Host-Bacterial Mutualism in the Human Intestine. *Science* **2005**, *307*, 1915–1920. [CrossRef] [PubMed]
2. Davidson, G.L.; Wiley, N.; Cooke, A.C.; Johnson, C.N.; Fouhy, F.; Reichert, M.; de la Hera, I.; Crane, J.M.S.; Kulahci, I.G.; Ross, R.P.; et al. Diet induces parallel changes to the gut microbiota and problem solving performance in a wild bird. *Sci. Rep.* **2019**, *10*, 20783. [CrossRef] [PubMed]
3. Shapira, M. Gut Microbiotas and Host Evolution: Scaling Up Symbiosis. *Trends Ecol. Evol.* **2016**, *31*, 539–549. [CrossRef] [PubMed]
4. Waite, D.W.; Taylor, M.W. Characterizing the avian gut microbiota: Membership, driving influences, and potential function. *Front. Microbiol.* **2014**, *5*, 223. [CrossRef]
5. Hird, S.M. Evolutionary Biology Needs Wild Microbiomes. *Front. Microbiol.* **2017**, *8*, 725. [CrossRef]
6. García-Amado, M.A.; Shin, H.; Sanz, V.; Lentino, M.; Domínguez-Bello, M.G. Comparison of gizzard and intestinal microbiota of wild neotropical birds. *PLoS ONE* **2018**, *13*, e0194857. [CrossRef]
7. Laviad-Shitrit, S.; Izhaki, I.; Lalzar, M.; Halpern, M. Comparative Analysis of Intestine Microbiota of Four Wild Waterbird Species. *Front. Microbiol.* **2019**, *10*, 1911. [CrossRef]
8. Videvall, E.; Ruiz-Limón, P.; Martínez-Padilla, J.; Moreno-Indias, I.; Canal, D.; Muriel, J. Fine-scale variation in the gut microbiome of the European pied flycatcher (*Ficedula hypoleuca*) in central Spain. *Ardeola* **2025**, *73*, 23–42. [CrossRef]
9. Maraci, Ö.; Antonatou-Papaioannou, A.; Jünemann, S.; Castillo-Gutiérrez, O.; Busche, T.; Kalinowski, J.; Caspers, B.A. The gut microbial composition is species-specific and individual-specific in two species of estrildid finches, the Bengalese finch and the zebra finch. *Front. Microbiol.* **2021**, *12*, 619141. [CrossRef]
10. Liukkonen, M.; Muriel, J.; Martínez-Padilla, J.; Nord, A.; Pakanen, V.M.; Rosivall, B.; Tilgar, V.; van Oers, K.; Grond, K.; Ruuskanen, S. Seasonal and environmental factors contribute to the variation in the gut microbiome: A large-scale study of a small bird. *J. Anim. Ecol.* **2024**, *93*, 1475–1492. [CrossRef]
11. Bodawatta, K.H.; Kleková, I.; Kleka, J.; Puejová, K.; Koane, B.; Poulsen, M.; Jønsson, K.A.; Sam, K. Specific gut bacterial responses to natural diets of tropical birds. *Sci. Rep.* **2022**, *12*, 713. [CrossRef] [PubMed]
12. Li, Z.T.; Duan, T.F.; Wang, L.; Wu, J.W.; Meng, Y.J.; Bao, D.L.; Gao, L.; Liu, L. Comparative analysis of the gut bacteria and fungi in migratory demoiselle cranes (*Grus virgo*) and common cranes (*Grus grus*) in the Yellow River Wetland, China. *Front. Microbiol.* **2024**, *15*, 1341512. [CrossRef] [PubMed]
13. Liu, J.P.; Li, L.Q.; Shao, Y.; Li, W.J.; Li, Y.Z.; Wang, H.G.; Wang, Y.; Zhou, Z.; Wang, J.; Shang, S. Comparative analysis of intestinal flora community composition and diversity of *Anas platyrhynchos* and *Anser fabalisin* the Yellow River Delta. *Anim. Biol.* **2024**, *74*, 435–451. [CrossRef]
14. Bolyen, E.; Rideout, J.R.; Dillon, M.R.; Bokulich, N.A.; Abnet, C.C.; Al-Ghalith, G.A.; Alexander, H.; Alm, E.J.; Arumugam, M.; Asnicar, F. Reproducible, interactive, scalable and extensible microbiome data science using QIIME 2. *Nat. Biotechnol.* **2019**, *37*, 852–857. [CrossRef]
15. Callahan, B.J.; Mcmurdie, P.J.; Rosen, M.J.; Han, A.W.; Johnson, A.; Holmes, S.P. DADA2: High-resolution sample inference from Illumina amplicon data. *Nat. Methods* **2016**, *13*, 581–583. [CrossRef]
16. Grice, E.A.; Kong, H.H.; Conlan, S.; Deming, C.B.; Davis, J.; Young, A.C.; NISC Comparative Sequencing Program; Bouffard, G.G.; Blakesley, R.W.; Murray, P.R.; et al. Topographical and temporal diversity of the human skin microbiome. *Science* **2009**, *324*, 1190–1192. [CrossRef]
17. Dubois, P.C.; Trynka, G.; Franke, L.; Hunt, K.A.; Romanos, J.; Curtotti, A.; Zhernakova, A.; Heap, G.A.; Adány, R.; Aromaa, A.; et al. Multiple common variants for celiac disease influencing immune gene expression. *Nat. Genet.* **2010**, *42*, 295–302. [CrossRef]
18. Hird, S.M.; Carstens, B.C.; Cardiff, S.W.; Dittmann, D.L.; Brumfield, R.T. Sampling locality is more detectable than taxonomy or ecology in the gut microbiota of the brood-parasitic Brown-headed Cowbird (*Molothrus ater*). *PeerJ* **2014**, *2*, e321. [CrossRef]
19. Fuirst, M.; Veit, R.; Hahn, M.; Dheilly, N.; Thorne, L.H. Effects of urbanization on the foraging ecology and microbiota of the generalist seabird *Larus argentatus*. *PLoS ONE* **2018**, *13*, e0209200. [CrossRef]
20. Dong, Y.; Xiang, X.; Zhao, G.; Song, Y.; Zhou, L. Variations in gut bacterial communities of hooded crane (*Grus monacha*) over spatial-temporal scales. *PeerJ* **2019**, *7*, e7045. [CrossRef]
21. Xiang, X.; Zhang, F.; Fu, R.; Yan, S.; Zhou, L. Significant Differences in Bacterial and Potentially Pathogenic Communities Between Sympatric Hooded Crane and Greater White-Fronted Goose. *Front. Microbiol.* **2019**, *10*, 163. [CrossRef] [PubMed]
22. Song, S.J.; Sanders, J.G.; Delsuc, F.; Metcalf, J.; Amato, K.; Taylor, M.W.; Mazel, F.; Lutz, H.L.; Winker, K.; Graves, G.R.; et al. Comparative Analyses of Vertebrate Gut Microbiomes Reveal Convergence between Birds and Bats. *mBio* **2020**, *11*, e02901-19. [CrossRef] [PubMed]
23. Zhao, J.S.; Wang, Y.J.; Zhang, M.; Yao, Y.F.; Tian, H.; Sang, Z.L.; Wang, L.; Xu, H. Structural changes in the gut microbiota community of the black-necked crane (*Grus nigricollis*) in the wintering period. *Arch. Microbiol.* **2021**, *203*, 6203–6214. [CrossRef] [PubMed]

24. Davidson, G.L.; Somers, S.E.; Wiley, N.; Johnson, C.N.; Reichert, M.S.; Ross, R.P.; Stanton, C.; Quinn, J.L. A time-lagged association between the gut microbiome, nestling growth and nestling survival in wild great tits. *Cold Spring Harb. Lab.* **2020**, *90*, 989–1003.
25. Cho, H.; Lee, W.Y. Interspecific comparison of the fecal microbiota structure in three *Arctic migratory bird* species. *Ecol. Evol.* **2020**, *10*, 5582–5594. [CrossRef]
26. Pepke, M.L.; Hansen, S.B.; Limborg, M.T. Unraveling host regulation of gut microbiota through the epigenome-microbiome axis. *Trends Microbiol.* **2024**, *32*, 1229–1240. [CrossRef]
27. Flint, H.J.; Bayer, E.A.; Rincon, M.T.; Lamed, R.; White, B.A. Polysaccharide utilization by gut bacteria: Potential for new insights from genomic analysis. *Nat. Rev. Microbiol.* **2008**, *6*, 121–131. [CrossRef]
28. Wu, H.; Wu, F.T.; Zhou, Q.H.; Zhao, D.P. Comparative Analysis of Gut Microbiota in Captive and Wild Oriental White Storks: Implications for Conservation Biology. *Front. Microbiol.* **2021**, *12*, 649466. [CrossRef]

Disclaimer/Publisher's Note: The statements, opinions and data contained in all publications are solely those of the individual author(s) and contributor(s) and not of MDPI and/or the editor(s). MDPI and/or the editor(s) disclaim responsibility for any injury to people or property resulting from any ideas, methods, instructions or products referred to in the content.